OXFORD

Human Molecular Genetics, 2018, Vol. 27, No. 1 95–106

doi: 10.1093/hmg/ddx387
Advance Access Publication Date: 2 November 2017
Original Article

ORIGINAL ARTICLE

Loss of *Drosophila* FMRP leads to alterations in energy metabolism and mitochondrial function

Eliana D. Weisz[1], Atif Towheed[2], Rachel E. Monyak[1], Meridith S. Toth[1], Douglas C. Wallace[1,2,3] and Thomas A. Jongens[1,*]

[1]Department of Genetics, Perelman School of Medicine at the University of Pennsylvania, Philadelphia, PA 19104, USA, [2]Center for Mitochondrial and Epigenomic Medicine, The Children's Hospital of Philadelphia, Philadelphia, PA 19104, USA and [3]Department of Pathology and Laboratory Medicine, University of Pennsylvania, Philadelphia, PA 19104, USA

*To whom correspondence should be addressed at: Department of Genetics, Perelman School of Medicine at the Univeristy of Pennsylvania, 10-134 Civic Center Boulevard, Building 421, Philadelphia, PA 19104, USA. Tel: +1 2155739332; Fax: +1 2155739411; Email: jongens@pennmedicine.upenn.edu

Abstract

Fragile X Syndrome (FXS), the most prevalent form of inherited intellectual disability and the foremost monogenetic cause of autism, is caused by loss of expression of the *FMR1* gene . Here, we show that *dfmr1* modulates the global metabolome in *Drosophila*. Despite our previous discovery of increased brain insulin signaling, our results indicate that *dfmr1* mutants have reduced carbohydrate and lipid stores and are hypersensitive to starvation stress. The observed metabolic deficits cannot be explained by feeding behavior, as we report that *dfmr1* mutants are hyperphagic. Rather, our data identify *dfmr1* as a regulator of mitochondrial function. We demonstrate that under supersaturating conditions, *dfmr1* mutant mitochondria have significantly increased maximum electron transport system (ETS) capacity. Moreover, electron micrographs of indirect flight muscle reveal striking morphological changes in the *dfmr1* mutant mitochondria. Taken together, our results illustrate the importance of *dfmr1* for proper maintenance of nutrient homeostasis and mitochondrial function.

Introduction

Fragile X Syndrome (FXS) is the most common heritable form of intellectual impairment and the leading monogenetic cause of autism, with a prevalence of 1 in 4000 males and 1 in 6000 females (1,2). At the molecular level, FXS arises primarily due to a noncoding CGG-trinucleotide repeat in the 5' untranslated region (UTR) of the fragile X mental retardation 1 (*FMR1*) gene (3). In affected individuals, *FMR1* contains over 200 CGG repeats, which results in hypermethylation of the locus and subsequent transcriptional silencing of the *FMR1* gene (4–6). Consequently, this pathogenic mutation eliminates the expression of the product of the *FMR1* gene, termed Fragile X Mental Retardation Protein (FMRP), which is an RNA binding protein that is thought to act primarily as a translational regulator (7–12).

In addition to intellectual disability, FXS patients present with several behavioral and cognitive symptoms including attention deficit disorder, sleep disorders, seizures, and an array of autism-associated behaviors (2,13,14). Several irregular physical features have also been observed in affected individuals such as altered facial structure, prominent ears, high-arched palate, hyperflexible joints, and macro-orchidism in post-pubertal males (13,15–17). Moreover, reports in the clinical literature have suggested that individuals, particularly children, with FXS show signs of metabolic dysfunction. Children with

Received: June 6, 2017. **Revised:** September 22, 2017. **Accepted:** October 25, 2017

FXS have been reported to have higher rates of obesity than the general population (18). Further, there have been several documented cases of affected individuals who exhibit hyperphagia and a lack of satiation after meals (19,20). This suite of symptoms has been termed the Prader-Willi Phenotype of FXS due to the substantial phenotypic similarity between the two conditions (19,21). The Prader-Willi Phenotype of FXS appears to be particularly relevant on a behavioral and cognitive level, as affected individuals who present with the Prader-Willi Phenotype have more severe behavioral problems and a higher rate of autism than that typically seen in FXS patients (22–25). Despite these remarkable findings, there is a dearth of studies that assess metabolic function in FXS patients or animal models of the disease.

One model that has emerged as a valuable tool to study FXS pathogenesis is *Drosophila melanogaster*. The *Drosophila* genome contains a single ortholog of *FMR1*, termed *dfmr1*, the product of which shares a high degree of sequence identity and biochemical properties with members of the FMR protein family (26). Extensive research has shown that flies with loss-of-function mutations in the *dfmr1* gene display phenotypic abnormalities that are remarkably similar to those observed in human patients, including abnormal synapse structure, learning and memory defects, altered circadian rhythms, and social behavioral deficits (27–29). Recently, the dysregulation of insulin signaling has been implicated in disease pathology in the *Drosophila* model of FXS (30). Several components of the insulin signaling pathway were found to be increased in the brains of *dfmr1* mutant flies (30). These observations led to the striking discovery that genetically reducing insulin signaling is sufficient to increase circadian rhythmicity and rescue learning and memory deficits in *dfmr1* mutant flies (30). Since proper regulation of insulin signaling is critical to maintain metabolic homeostasis, we hypothesized that metabolism would be perturbed in the *dfmr1* mutant flies.

Results

dfmr1 regulates global metabolism

To understand the role of dFMRP in the regulation of metabolic homeostasis we began with a broad, unbiased approach. Specifically, we asked whether we could detect differences in the global metabolome of flies with a loss-of-function mutation in the *dfmr1* gene relative to *iso31Bw-* (wild-type) conspecifics. As an additional control, we also included transgenic flies that contain a wild-type copy of the *dfmr1* gene that has been inserted on another chromosome in a genetic background that is otherwise *dfmr1* mutant, termed wild-type rescue (WTR) flies (28). Given that metabolism in *Drosophila* is modulated by circadian clocks, all flies were entrained on a strict 12: 12 light: dark (LD) cycle (31,32). Moreover, to avoid any potential confounds due to age or gender, we limited our studies to 5- to 7-day-old male flies. The 5- to 7-day age range was of particular interest to us because it is the age at which there are known neuroanatomical alterations and impairments in behavior and cognition (28,29).

Samples comprised of 50 whole flies per genotype were extracted and loaded onto an ultrahigh performance liquid chromatography-tandem mass spectroscopy (UPLC-MS/MS) platform for global metabolic profiling. We then utilized Principle Component Analysis (PCA) on the resultant datasets to determine whether it was possible to segregate samples of each genotype based solely on differences in their overall metabolite signature. Congruent with our hypothesis that global metabolism is altered in the absence of dFMRP, PCA analysis revealed a distinct separation between the *dfmr1* mutant, wild-type, and WTR flies (Supplementary Material, Fig. S1). The minimal overlap between the groups of 5 independent biological replicates of each genotype indicates that there is indeed a significant shift in the biochemical signature of the *dfmr1* mutant flies relative to the wild-type and WTR controls. This novel finding suggests that in *Drosophila*, the loss of dFMRP substantially influences organismal physiology. Our data are consistent with a previous report that the brains of *Fmr1* null mice exhibit a distinct metabolic signature (33). Remarkably, the murine study also demonstrated that various brain regions are differentially affected by the absence of FMRP (33). Taking the exquisite spatiotemporal specificity of FMRP function alongside evidence of insulin signaling dysregulation in *dfmr1* mutants (30), we decided to further probe metabolic alterations in the context of the periphery.

Carbohydrate metabolism is deficient in the absence of *dfmr1*

Encouraged that we successfully identified global differences in the metabolome of the *dfmr1* mutants, our next objective was to probe differences in specific subgroups of metabolites. Based upon our previous finding that insulin signaling is elevated in the brain of *dfmr1* mutants, we were particularly eager to evaluate changes in carbohydrate metabolism (30). Since proper regulation of insulin signaling is critical to maintain glucose homeostasis in mammals and *Drosophila* (34–37), we hypothesized that glucose levels would be altered in the *dfmr1* mutants. Our metabolomics data indicate that glucose levels are dramatically decreased in the *dfmr1* mutants relative to their wild-type and WTR counterparts (Fig. 1A and B; Supplementary Material, Table S1). Moreover, we saw a similar decrease in glucose 6-phosphate levels (Fig. 1C, Supplementary Material, Table S1).

To further explore alterations in carbohydrate metabolism, we next measured glycogen levels in the bodies of *dfmr1* mutants and their wild-type and WTR counterparts. Glycogen, which is a storage polymer of glucose, is the primary form of carbohydrate storage in *Drosophila* (38). Consistent with the observed decrease in its precursors, glucose and glucose 6-phosphate, *dfmr1* mutants had drastically reduced levels of glycogen compared with the wild-type and WTR flies (Fig. 1D). These alterations cannot be accounted for by differences in body size, as the weight of *dfmr1* mutants is comparable to that of wild-type flies (Supplementary Material, Fig. S2). Moreover, notwithstanding the role of dFMRP as a translational regulator, we did not detect any differences in protein levels when we measured overall protein levels for normalization purposes (Supplementary Material, Fig. S2). Taken together, these results indicate that *dfmr1* is a necessary regulator of carbohydrate metabolism.

dfmr1 modulates lipid metabolism

Next, we chose to investigate potential differences in lipid metabolism. Recently, lipids have emerged as a target of interest in FXS (39–43). Contrary to the predominate view in the field that FMRP acts as a promiscuous RNA binding protein, data from a novel cross-linking immunoprecipitation (CLIP) study suggest that FMRP preferentially associates with one mRNA target, diacylglycerol kinase kappa (dgk_K), in cultured murine

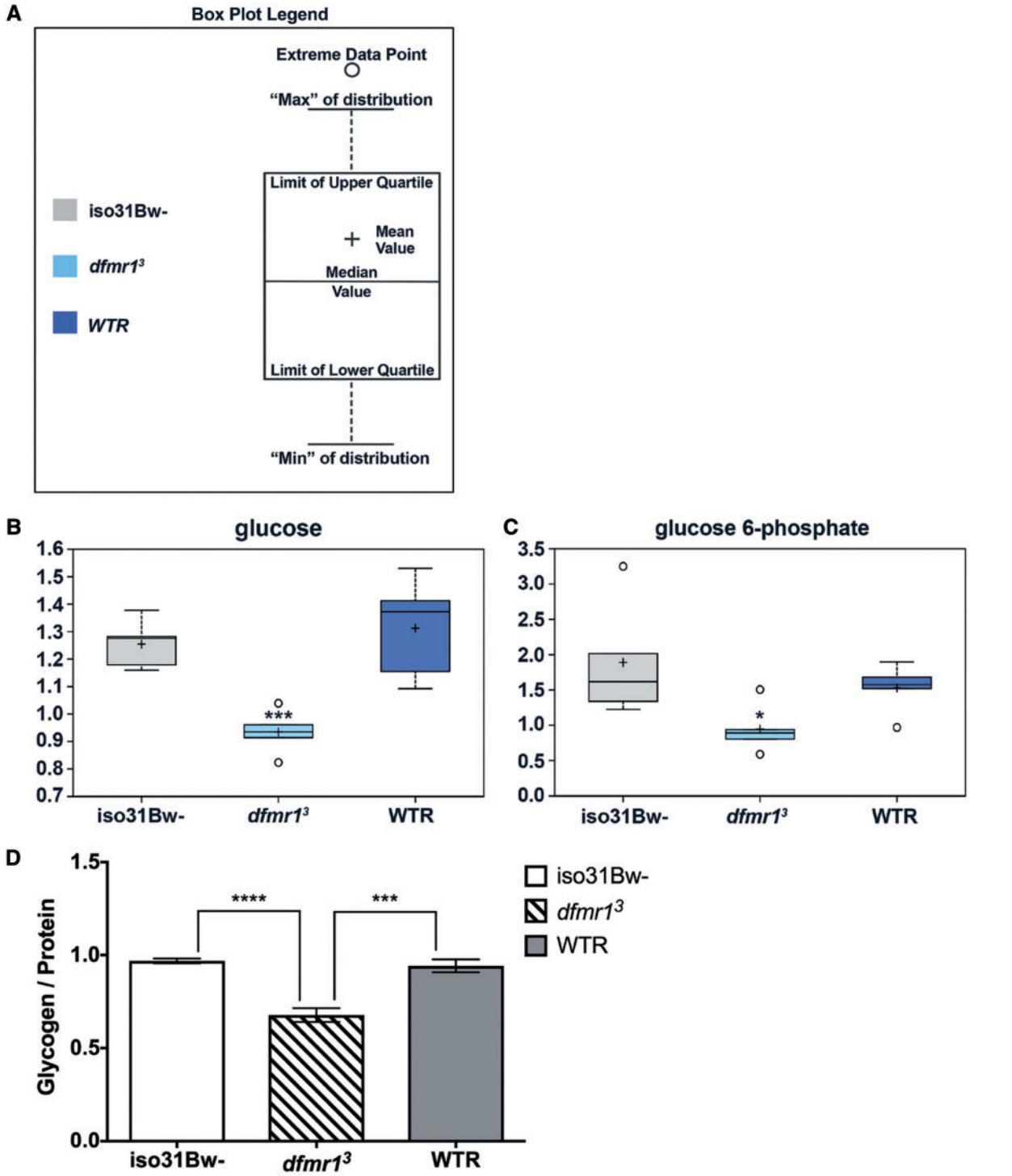

Figure 1. Carbohydrate levels are decreased in *dfmr1* mutant flies. (**A–C**) (**A**) Box plot legend, (**B**) quantification of glucose, and (**C**) glucose 6-phosphate levels in 5 independent biological replicates of each genotype. Box plots depict the scaled intensity value of each metabolite on the y-axis. Genotype is denoted on the x-axis. (**D**) Glycogen levels were measured in 5- to 7-day-old male flies of different genotypes. The resultant values were then normalized to protein content. Fly heads were removed prior to homogenization. Sample number (*N*) per genotype = 5. Each sample contained an independent group of 4 fly bodies. One-way ANOVAs revealed a significant group effect for glycogen ($P < 0.0001$). Post hoc Tukey tests indicated that *dfmr1* mutant flies had reduced levels of glycogen compared with iso31Bw- and WTR flies. Values represent mean ± SEM. ***$P \leq 0.001$, ****$P \leq 0.0001$.

cortical neurons (11,39). On a functional level, this contentious finding was reinforced by the discovery that human FMRP exhibited the highest binding affinity for the dgk_k transcript *in vitro* (39). Given that DGK_K modulates the balance between diacylglycerol and phosphatidic acid, both of which are critical components of membrane architecture and essential signaling molecules, the consequences of deregulation of DGK_K could contribute substantially to FXS etiology (39,42,43).

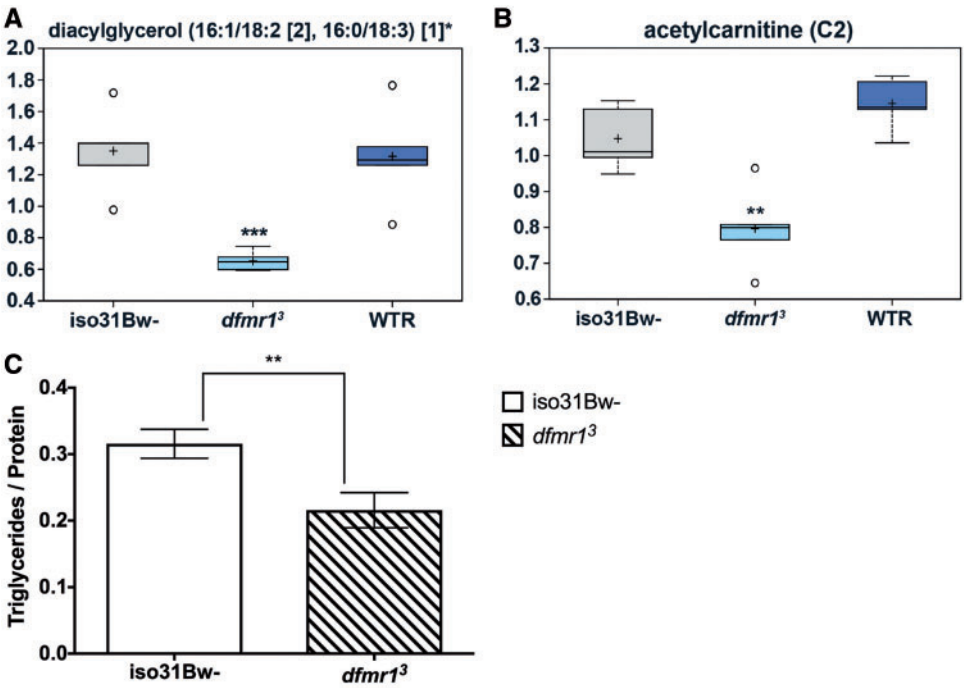

Figure 2. Lipid metabolites are diminished in *dfmr1* mutant flies. (**A,B**) (**A**) Representative box plot of diacylglycerol and (**B**) carnitine-conjugated lipid levels in 5 independent biological replicates of each genotype. Box plots depict the scaled intensity value of each metabolite on the y-axis. Genotype is denoted on the x-axis. (**C**) Triglyceride levels were measured in 5- to 7-day-old male flies of different genotypes. The resultant values were then normalized to protein content. Fly heads were removed prior to homogenization. Sample number (N) per genotype: iso31Bw- = 35, $dfmr1^3 = 29$. Each sample contained 1 fly body. Mann–Whitney test results indicated that *dfmr1* mutant flies had reduced levels of triglycerides compared with iso31Bw- flies ($P = 0.0061$). Data shown represent the cumulative results of 3 independent experiments. Values represent mean ± SEM. $^{**}P \leq 0.01$, $^{***}P \leq 0.001$.

Our whole-body metabolomics study in 5- to 7-day-old flies detected significant reduction in 9 out of the 12 species of diacylglycerols measured in the *dfmr1* mutants relative to the wild-type and WTR controls (Fig. 2A, Supplementary Material, Fig. S3 and Table S1). Notably, these findings contradict the report of an increase in several species of diacylglycerols in cortical neuronal cultures derived from *Fmr1* knockout mouse embryos and cerebellar extracts from human FXS patients (39). This dichotomy emphasizes the notion that the loss of FMRP might precipitate differential effects depending upon spatiotemporal context. In addition to diacylglycerols, we also observed a decline in carnitine-conjugated lipids in the *dfmr1* mutants (Fig. 2B, Supplementary Material, Fig. S4 and Table S1). These findings are notable because deleterious variants of genes involved in carnitine biosynthesis have been implicated in sporadic autism (44,45).

Due to solubility constraints, we were unable to measure triglyceride levels in our metabolomics study. Triglycerides, which represent over 90% of stored lipids in *Drosophila*, have been shown to be tightly regulated by insulin signaling (34,36–38). Thus, to augment our metabolomics findings, we used another colorimetric assay to measure triglycerides in the bodies of *dfmr1* mutant and control flies. Consistent with the observed decrease in diacylglycerols, we found that peripheral triglyceride levels were significantly reduced in *dfmr1* mutants relative to wild-type controls (Fig. 2C). This finding is congruent with the observed decrease in glycogen levels (Fig. 1D) and indicates that the *dfmr1* mutants have greatly diminished carbohydrate and lipid stores.

Absence of *dfmr1* increases sensitivity to starvation

Next, we wanted to evaluate the functional implications of the observed reduction in energy stores. The ability to survive in the absence of nutrients is a robust paradigm to assess metabolic status, as starvation resistance is influenced by lipid and glycogen content (46–48). To measure the response of the *dfmr1* mutants and control flies to nutrient deprivation, we recorded the survival time of flies of each genotype on a 1% agar medium. Importantly, the 1% agar medium provided a uniform source of water such that any alterations in desiccation resistance did not confound our results (49). We found that the *dfmr1* mutants died much sooner than their wild-type and WTR counterparts when subjected to nutrient depravation. This result indicates that the *dfmr1* mutants are hypersensitive to starvation conditions (Fig. 3A). Presumably, the observed reduction in carbohydrate and lipid storage (Figs 1 and 2) renders the *dfmr1* mutant flies less resistant to starvation conditions.

dfmr1 regulates feeding behavior

The observed reductions in carbohydrates, lipids, and starvation resistance are the opposite of what we would expect to find under conditions of elevated insulin signaling (35,36). Rather, our results suggest that the metabolic disturbances that occur in the absence of *dfmr1* cannot be attributed to canonical insulin signaling hyperactivity. Intrigued by this dichotomy, we sought to better understand the mechanisms underlying the observed metabolic differences.

The first hypothesis that we tested was the possibility that the *dfmr1* mutants are hyperactive and thereby deplete their available carbohydrate and lipid stores. To quantitate the average daily activity of *dfmr1* mutant and wild-type flies, we used the *Drosophila* Activity Monitoring (DAM) System. We found that the average daily activity of the *dfmr1* mutants was comparable to that of the wild-type flies in the presence of light: dark cues

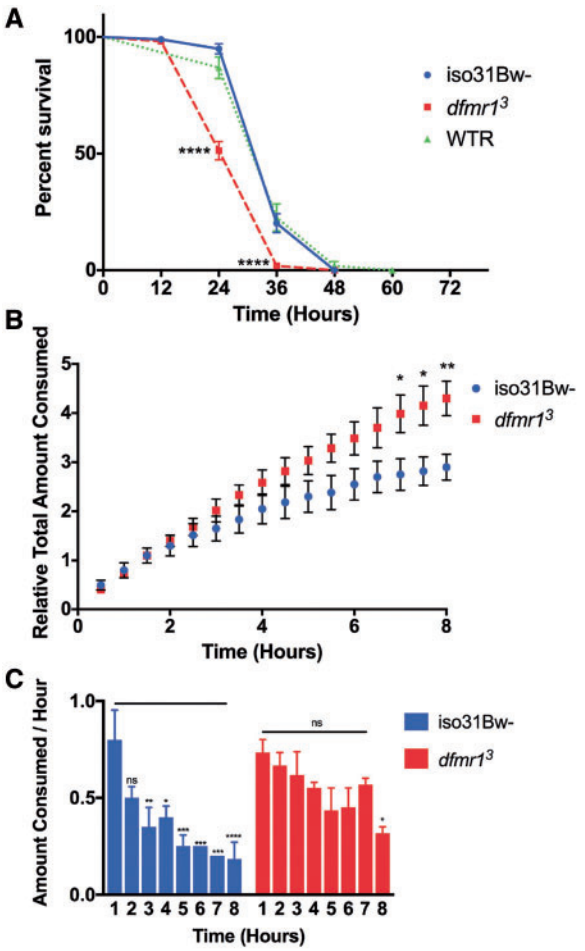

Figure 3. *dfmr1* mutant flies are more sensitive to starvation conditions despite hyperphagia. (**A**) Starvation resistance was measured by recording the average survival time of 5- to 7-day-old males of each genotype on media containing 0% sucrose and 1% agar. Sample number (*N*) per genotype: iso31Bw-=99, $dfmr1^3$=160, WTR=53. Log-rank (Mantel-Cox) test results indicated that *dfmr1* mutants were less resistant to starvation than the iso31Bw- ($P \leq 0.0001$) and WTR ($P \leq 0.0001$) flies. (**B**) The total amount of 100 mM sucrose consumed was measured every 30 minutes. All values recorded were then normalized to an evaporation control. Sample number (*N*) per genotype = 3. Each sample contained an independent group of 35 flies. Two-way ANOVA found that the interaction between the relative total amount consumed and genotype to be significant ($p < 0.0001$). Asterisks denote significant differences in the relative consumption of *dfmr1* mutants compared with that of the iso31Bw- flies as determined using Sidak's multiple comparison test. (**C**) Hourly consumption was determined by subtracting the total consumption from the preceding hour from the total consumption each hour. Two-way ANOVA found that for both genotypes, the interaction between the amount consumed and time to be significant ($P < 0.0001$). Statistical significance for the amount consumed each hour compared with consumption during the first hour of the assay was determined using Sidak's multiple comparison test. Values represent mean ± SEM. $^{*}P \leq 0.05$, $^{**}P \leq 0.01$, $^{***}P \leq 0.001$, $^{****}P < 0.0001$.

(Supplementary Material, Fig. S5). Thus, we concluded that activity levels do not contribute substantially to the observed metabolic changes.

Subsequently, we turned to feeding behavior to ascertain clues about the mechanistic underpinnings of the observed metabolic deficits. We used the well-established capillary feeder (CAFE) assay to quantitate the amount of 100 mM sucrose consumed by the *dfmr1* mutant and wild-type flies. To induce detectable changes in feeding over time, we first starved flies for 12 h on 1% agar. The 12 h duration was selected because it is the time at which feeding behavior is driven by taste-independent mechanisms such that any differences in taste ability or preferences would not confound our results (50). The flies were then allowed to feed *ad libitum* on a highly appetitive 100 mM sucrose solution until this food source was exhausted. Our results indicate that initially total consumption was not significantly different between genotypes, which was not too surprising given that the prior 12 h of starvation rendered both groups of flies primed to feed. However, as time progressed the *dfmr1* mutants diverged significantly from their wild-type counterparts and consumed much more of the 100 mM sucrose (Fig. 3B). This striking discovery prompted us to delve deeper into the temporal dynamics of feeding behavior. To assess the feeding pattern of the *dfmr1* mutant and wild-type flies, we quantified the amount of 100 mM sucrose consumed by each genotype every hour. This analysis revealed that the wild-type flies ate the most during the first 2 h of the assay and subsequently decreased feeding for the remainder of the assay (Fig. 3C). In contrast, the *dfmr1* mutants sustained a high level of consumption for 7 h followed by a modest reduction in feeding for the last hour of the assay (Fig. 3C). Taken together, it appears that after acute starvation the *dfmr1* mutants are unable to become sated and suppress feeding like their wild-type counterparts. This novel finding is highly reminiscent of reports in the clinical literature of FXS patients that fail to achieve satiety and instead eat to excess (22,23,25).

dfmr1 is important for mitochondrial function

Since the observed metabolic differences could not be explained by activity levels or feeding behavior, we speculated that mitochondrial dysfunction could contribute to FXS pathogenesis in our *Drosophila* model. In support of this hypothesis, our metabolomics data suggest that nicotinamide adenine dinucleotide (NAD) metabolism is regulated by *dfmr1*. Specifically, we found that both nicotinic acid adenine dinucleotide ($NAAD^+$) and NAD^+ levels were greatly diminished in the *dfmr1* mutants relative to the wild-type and WTR control flies (Fig. 4A–C, 4F, Supplementary Material, Table S1). Importantly, the concomitant reduction of $NAAD^+$ and NAD^+ suggests that NAD biosynthesis is impaired in the *dfmr1* mutants. This deficiency is particularly problematic given that that availability of NAD^+ is pivotal for proper mitochondrial function, as mitochondrial ATP production and membrane potential require NAD^+ as a cofactor (51). As such, the observed decrease in $NAAD^+$ and NAD^+ levels in the absence of *dfmr1* could have deleterious consequences for mitochondrial bioenergetics.

To delve deeper into changes in NAD metabolism, we subsequently measured the NAD^+/NADH ratio. During the tricarboxylic acid (TCA) cycle, NAD^+ gains two electrons and a proton, thereby being reduced to NADH (Fig. 4F). In turn, the NADH generated is oxidized upon the donation of the electrons gained to the electron transport chain (ETC). The reliance of the TCA cycle and the ETC on NAD^+ and NADH, respectively, underscores the importance of the maintenance of the optimal NAD^+/NADH ratio for mitochondrial function. Based upon this knowledge and our finding that NAD^+ levels are reduced in the *dfmr1* mutants (Fig. 4B and F), we hypothesized that the absence of dFMRP would result in an altered NAD^+/NADH ratio. Consistent with our metabolomics data, we observed a significant decrease in the levels of NAD^+ in the *dfmr1* mutants. We also observed that NADH levels were significantly augmented in the *dfmr1* mutants (Fig. 4D and

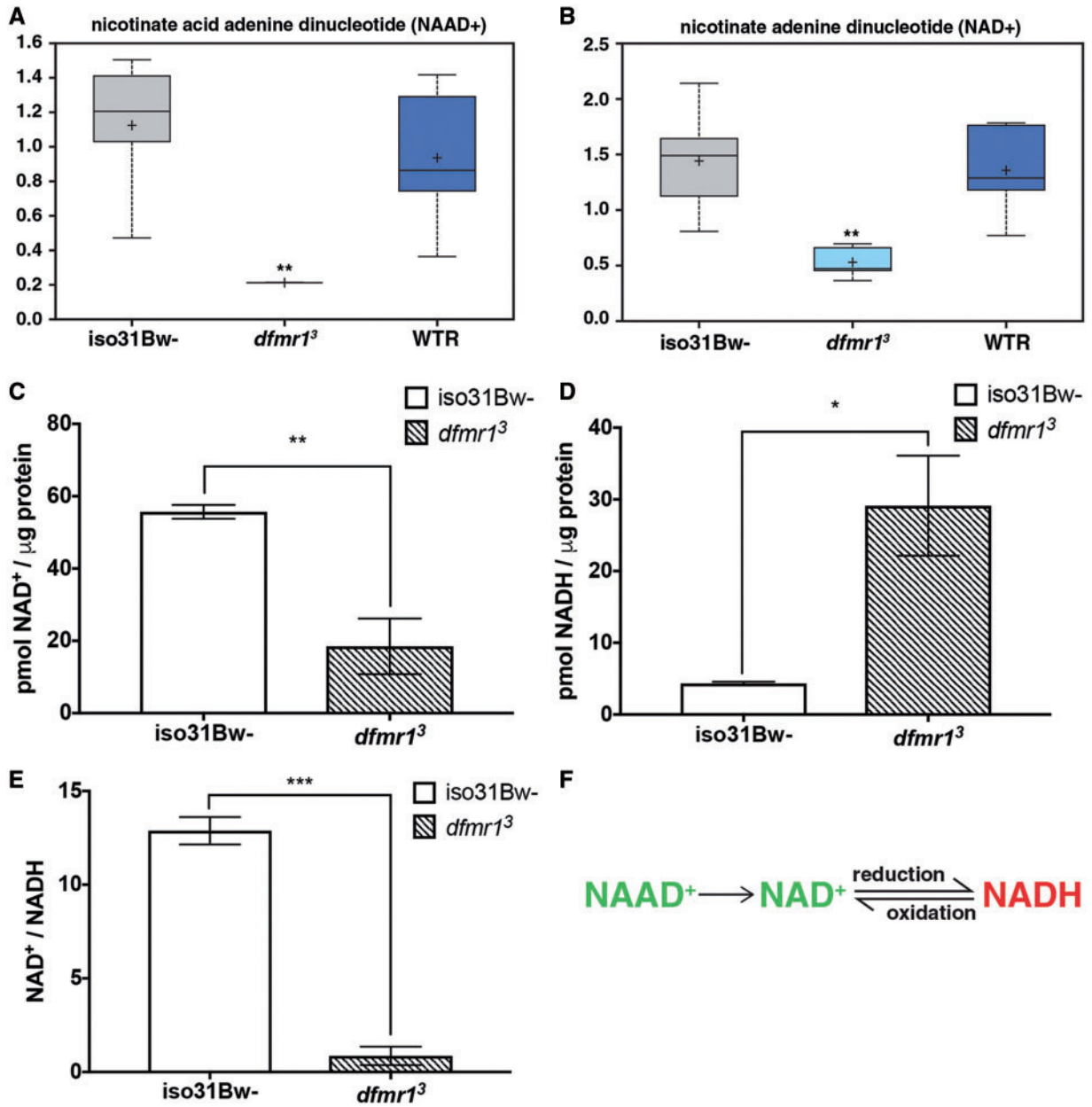

Figure 4. NAD metabolism is reduced in *dfmr1* mutant flies. (**A,B**) (A) Quantification of $NAAD^+$ and (**B**) NAD^+ levels in 5 independent biological replicates of each genotype. Box plots depict the scaled intensity value of each metabolite on the y-axis. Genotype is denoted on the x-axis. (**C–E**), (**C**) Quantification of NAD^+, (**D**) NADH, and (E) NAD^+/NADH ratio. The levels of NAD^+ and NADH were normalized to protein content. Each sample contained 10 fly bodies. Sample number (N) per genotype = 3. Unpaired *t*-tests indicated that NAD^+ levels were significantly diminished ($P = 0.0094$), NADH levels were significantly elevated ($P = 0.0238$), and the NAD^+/NADH ratio was significantly lower ($P = 0.0002$) in the *dfmr1* mutants relative to iso31Bw- controls. (**F**) Schematic illustrating the relationship between $NAAD^+$, NAD^+, and NADH. Green type signifies biochemicals that were lower in the *dfmr1* mutants compared with control flies. Red type indicates a biochemical that was augmented in the *dfmr1* mutants relative to control flies. Values represent mean ± SEM. $^*P \leq 0.05$, $^{**}P \leq 0.01$, $^{***}P \leq 0.001$.

F). The combined diminution of NAD^+ levels and elevation of NADH levels results in a dramatically reduced NAD^+/NADH ratio in the *dfmr1* mutants compared with wild-type flies (Fig. 4E and H). Thus, while we do see indications of impaired NAD^+ biosynthesis, the accumulation of NADH suggests that there may be multiple defects in NAD metabolism (Fig. 4F).

In further support of the notion that mitochondrial metabolism is altered in the absence of dFMRP, it has been shown that *dfmr1* is a negative regulator of microtubule dependent mitochondrial transport (52). Thus, we reasoned that mitochondrial function would be altered in the *dfmr1* mutant flies. To explore this possibility, we performed high-resolution respirometry (HRR) on fresh thoracic mitochondrial preparations from *dfmr1* mutants and wild-type flies. We utilized the substrate-uncoupler-inhibitor titration (SUIT) protocol, which allows for real-time interrogation of mitochondrial oxygen flux (53,54). We found that when *dfmr1* mutant mitochondria were chemically uncoupled from the ATP synthase and provided with high levels of mitochondrially permeable organic substrates, their *in vitro* maximum electron transport system (ETS) capacity was

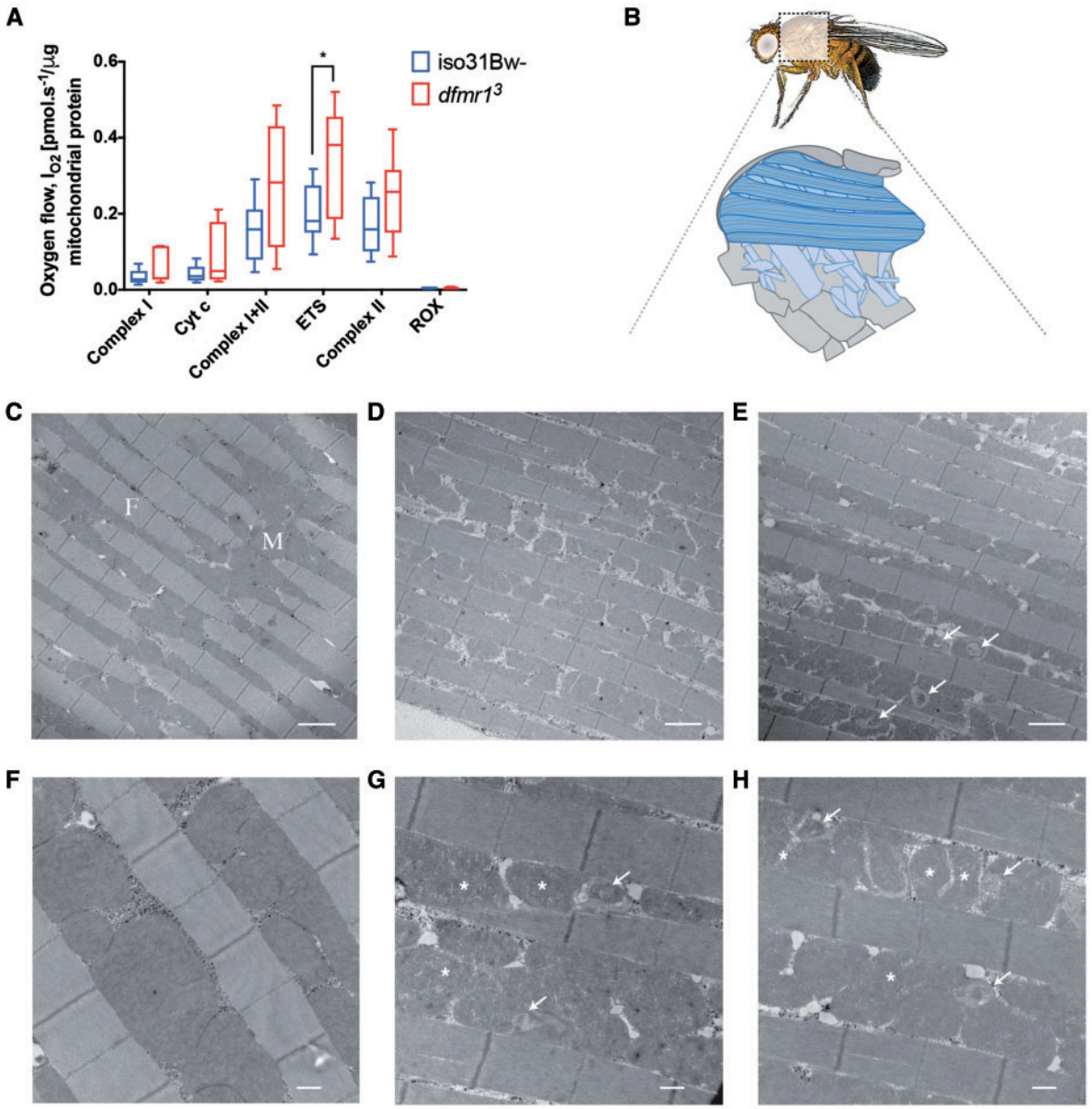

Figure 5. Mitochondrial function is altered in *dfmr1* mutant flies. (**A**) Oxygen flux was measured in mitochondrial preparations from fly thoraces and subsequently normalized to mitochondrial protein content. ETS was defined as the rate of oxygen consumption after the addition of FCCP. ROX represents the non-mitochondrial residual oxygen consumption rate after the addition of Rotenone and Antimycin. Sample number (N) per genotype for complex I, cytochrome c, complex I + II, ETS = 6 for both genotypes. Sample number (*N*) per genotype for ROX = 5 for both genotypes. Each sample was comprised of thoracic mitochondria isolated from 50 flies. Two-way ANOVA found the interaction between genotype and oxygen flux to be significant ($P = 0.0023$). Post hoc Sidak's multiple comparison test results indicated that ETS was significantly elevated in the *dfmr1* mutant flies compared with the iso31Bw- controls. Data shown represent the cumulative results of 6 independent experiments. Values represent mean ± SEM. *$P \leq 0.05$ (**B**) Longitudinal sections of indirect flight muscle were prepared from isolated thoraces (dashed box) for transmission electron microscopy experiments. The inset depicts a sagittal view of the thoracic musculature. Imaging was performed on the region illustrated in dark blue. (**C–E**), Electron micrographs of *Drosophila* flight muscle at 7, 500× magnification. (**C**) iso31Bw- and *dfmr1* mutant (**D**, **E**) mitochondria, M, are aligned between rows of myofibrils, (**F**) Scale bar indicates 2 microns. (**F–H**), Electron micrographs of *Drosophila* flight muscle at 20, 000× magnification. (**F**) iso31Bw- and *dfmr1* mutant (**G**,**H**) mitochondria at higher magnification. Scale bar indicates 500 nm. Arrows denote local disruptions in cristae. Asterisks signify marked dispersions of cristae.

elevated (Fig. 5A). This discovery was unexpected considering our NAD^+/NADH results (Fig. 4), as elevated electron transport would be expected to oxidize NADH to NAD^+.

While the observed increase in maximum ETS capacity appears to be inconsistent with our observation that the NAD^+/NADH ratio is diminished in the *dfmr1* mutants, we cannot rule out the possibility the methodology used in these experiments precluded our ability to detect such changes. Specifically, the NAD^+/NADH data cannot be directly compared the HRR results, as the HRR experiments were performed using mitochondrial extracts whereas the measurement of NAD^+/NADH levels was performed using whole-body lysates. Importantly, the pool of mitochondrial NAD^+ and NADH is kept separate from that of the cytosol (51). Given that the levels of NAD^+ and NADH are much higher in the cytosol than in mitochondria, the dramatic changes that we observe likely reflect alterations in cytosolic levels of NAD^+ and NADH (51). Further studies of the mitochondrial pool of NAD in the *dfmr1* mutants will be necessary to

reconcile the apparent discrepancy between our observations regarding NAD^+/NADH levels and maximum ETS capacity. An intriguing alternative explanation that merits rigorous examination is the possibility that the *dfmr1* mutants may have a defect in the ability to shuttle cytosolic NADH into the mitochondrion.

Consistent with a systemic defect in mitochondrial oxidative phosphorylation, transmission electron micrographs of the *dfmr1* mutant flight muscle mitochondrial revealed marked mitochondrial abnormalities (Fig. 5B–H). For this analysis, we prepared longitudinal sections of indirect flight muscle, as this tissue has high-energy demands that require robust mitochondrial function (55) (Fig. 5B). In the wild-type flies, we observed densely packed mitochondria evenly aligned with and distributed along the length of the adjacent myofibrils (Fig. 5C). However, the mitochondrial ultrastructure of the *dfmr1* mutants revealed severe pathology characterized by variable, frequently smaller mitochondria that were irregularly spaced (Fig. 5D). We also noticed that several of the *dfmr1* mutant mitochondria had aberrant membrane morphology (Fig. 5E). Images taken at higher magnification revealed that sections of the *dfmr1* mutant mitochondria had localized disruptions in the cristae (Fig. 5G and H). The loosely disbursed cristae in the *dfmr1* mutants were in sharp contrast to the densely packed cristae present in wild-type mitochondria (Fig. 5F). We believe that it is likely that these pathological lesions affect mitochondrial function.

Discussion

The findings presented here reveal major changes in metabolism and mitochondrial function in a *Drosophila* model of FXS. While the implications of the loss of *dfmr1* are canonically considered in the context of the brain, we have identified important physiological changes that occur at the systemic level in the absence of dFMRP. Here, we report a shift in the global metabolome of *dfmr1* mutant flies. Our metabolomics data along with the colorimetric quantification of glycogen and triglycerides provide compelling evidence that carbohydrates and lipids are dramatically reduced in the *dfmr1* mutants. These results are consistent with observation that that the body composition of *Fmr1/Fxr2* double knockout mice is characterized by reduced fat deposits as well as low plasma glucose, glycerol, free fatty acids, and cholesterol (56). Moreover, a retrospective study in a large cohort of adults with FXS found that total cholesterol (TC), low-density lipoprotein (LDL) and high density lipoprotein (HDL) were all significantly reduced in males with FXS relative to population normative data (40). Remarkably, this study concluded that unlike findings in the general population, there was no relationship between lipid levels and body mass index (BMI) (40). The lack of a relationship between lipid levels and BMI in the FXS cohort raises the possibility that the mechanism by which decreased lipid levels occur in FXS is independent of BMI. Importantly, the apparent evolutionary conservation of these deficits between flies, mice, and humans suggests that impairments in carbohydrate and lipid homeostasis are a robust feature of FXS pathophysiology.

In further support of our finding that energy stores are decreased in the *dfmr1* mutants, we also observed that *dfmr1* mutant flies exhibit augmented sensitivity to nutrient deprivation. Given that the ability to store and mobilize nutrients regulates the response to starvation conditions, it is likely that deficient energy storage underlies the diminished ability of the *dfmr1* mutants to withstand starvation conditions. Our efforts to determine the mechanistic underpinnings of the observed metabolic phenotypes lead to the striking discovery that food consumption is substantially elevated in the *dfmr1* mutant flies. Further, we identified a significant difference in feeding rate whereby unlike their wild-type counterparts, the *dfmr1* mutants fail to become sated and do not suppress feeding at later time points. Notably, a modest increase in *ad libitum* food intake was noted in *Fmr1/Fxr2* double knockout mice (56). However, the effect was much subtler than what we observed, likely because the static measurement of total daily food consumption precluded the ability to capture differences in feeding dynamics over time. Our results are particularly relevant on a translational level because the feeding phenotype that we identified in our *Drosophila* model is highly reminiscent of the Prader-Willi Phenotype of FXS. Given that there is a disproportionate prevalence of autism in FXS patients that present with the Prader-Willi Phenotype (22–25), we believe that we have identified a robust paradigm to evaluate the efficacy of certain therapeutic interventions on FXS and autism pathogenesis.

Given that mitochondria generate energy by oxidizing hydrogen supplied by carbohydrates and fats, the hyperphagy of the flies together with their reduced carbohydrate and lipid levels and stores indicate that mitochondrial dysfunction may contribute to the observed metabolic and physiological changes that arise in the absence of dFMRP. Congruent with this expectation, isolated flight muscle mitochondria from *dfmr1* mutant flies showed elevated maximal ETS capacity when chemically uncoupled from the ATP synthase *in vitro*. However, our observation that the NAD^+/NADH ratio is diminished in the *dfmr1* mutants is inconsistent with hyper-respiration. One potential explanation for this anomaly is the possibility that the *dfmr1* mutant flies have a defect in the ability to import reducing equivalents from cytosolic NADH into the mitochondrion. To address this hypothesis, further studies will be needed to characterize and evaluate possible alterations in NAD shuttling dynamics in the *dfmr1* mutant flies. Additionally, the apparent contradiction between the diminished ratio of NAD^+/NADH and the observed elevation of maximum ETS capacity in the *dfmr1* mutants provides a compelling foundation for follow-up studies to determine the directionality of changes in oxidative phosphorylation. This can be accomplished by measuring the expression and enzymatic activity levels of each component of the electron transport chain. It will also be critical to determine the levels of ATP in the *dfmr1* mutants to ascertain whether the mitochondria are effectively coupled. Without proper coupling, the utilization of reducing equivalents for electron transport would fail to yield commensurate levels of ATP.

Finally, we observed striking aberrations in the morphology of mitochondria in lateral sections of indirect flight muscle. Considering that mitochondrial ultrastructure and function are intimately linked, it is conceivable that the pathological changes that we uncovered could greatly impact energy production. In support of the notion that mitochondrial function is compromised in the absence of dFMRP, it has been shown previously that flight ability is impaired in *dfmr1* mutants (27).

The findings presented here raise several important questions regarding the ways in which dFMRP shapes the metabolic landscape. Notably, the extent to which mitochondrial dysfunction impinges on peripheral metabolism and the mechanisms by which dFMRP regulates these processes remain to be determined. In conclusion, our work combines metabolomic and physiological approaches to decipher novel roles of dFMRP and establish a foundation for studies of the ways in which metabolism and mitochondrial function contribute to the etiology of FXS and autism.

Materials and Methods

Fly genetics and husbandry

Fly strains that contain the *dfmr1*^{3} allele and WT *rescue* transgene are described in Dockendorff *et al*., (28). These flies were outcrossed to *w1118*(iso31Bw-) flies as described in Monyak *et al*., (30). The fly strains were cultured on a standard cornmeal-molasses medium and maintained in the presence of stringent 12 h light: 12 h dark (LD) cycles at 25 °C.

Metabolomics

5- to 7-day-old adult male flies were collected on dry ice. Flies of each genotype were pooled into five independent groups comprised of 50 flies. These samples were then sent for biochemical profiling at Metabolon, Inc., where they were extracted and prepared as described in Evans *et al*., (57). Briefly, the extract from each sample was divided into four fractions: one for analysis by UPLC-MS/MS with positive ion mode electrospray ionization, one for analysis by UPLC-MS/MS with negative ion mode electrospray ionization, one for analysis by GC-MS, and one sample was reserved for backup. Raw data were extracted, peak-identified, and QC processed using Metabolon's proprietary hardware and software. The resultant dataset was comprised of 373 compounds of known identity, termed named biochemicals. Following log transformation and, if necessary, imputation with minimum observed values for each compound, Welch's two-sample *t*-tests were used to detect biochemicals that differed significantly between each genotype.

Glycogen measurement

5- to 7-day-old adult male flies were collected on dry ice. Fly heads were removed prior to homogenization, as the presence of eye pigment can interfere with accurate absorbance measurements (49). The decapitated fly bodies were placed in groups of four and homogenized in 200 μl of 0.1M NaOH. The homogenate was then centrifuged at 15871 × *g* for 10 minutes at 4C°. The supernatant was extracted from each sample and 20 μl of the lysate was treated with 5 mg/ml Amyloglucosidase (Sigma-Aldrich, Saint Louis, MO) in 0.2 M acetate, pH 4.8, as this enzyme catabolizes glycogen to yield free glucose molecules. Concurrently, another 20 μl aliquot of the lysate was treated with 0.2 M acetate, pH 4.8 alone. Both reactions incubated for 2 h at 37°C. Subsequently, the free glucose content in each reaction was measured in triplicate with the Amplex Red Glucose/Glucose Oxidase Assay kit (Molecular Probes, Eugene, OR). The protein concentration of these reactions was then determined with the Pierce® BCA Protein Assay Kit (Thermo Scientific, Rockford, IL) for normalization. The glycogen content of each sample was calculated by subtracting the free glucose concentration of the untreated lysate from the free glucose concentration of the lysate that was treated with amyloglucosidase.

Triglyceride measurement

Triglyceride levels were measured as described in DiAngelo and Birnbaum (58). Briefly, individual 5- to 7-day-old adult male flies were collected on dry ice. Fly heads were removed prior to homogenization, as the presence of eye pigment can interfere with accurate absorbance measurements (49). The decapitated fly bodies were then homogenized in lysis buffer that contained 140mM NaCl, 50mM Tris-HCL, pH 7.4, 20% Triton X-100, and 1X protease inhibitors (Roche, Indianapolis, IN). The homogenate was then centrifuged at 15871 × *g* for 10 minutes at 4°C. Triglyceride concentrations were determined in triplicate with the Triglyceride LiquiColor kit (Stanbio Laboratory, Boerne, TX). The protein concentration of each sample was measured with the Pierce® BCA Protein Assay Kit (Thermo Scientific, Rockford, IL). The triglyceride concentration of each sample was then normalized to its respective protein content.

Starvation resistance

5- to 7-day-old adult male flies were reared on standard medium. These flies were subsequently transferred in groups of 20 to plastic vials that contained a 1% agar medium. All starvation vials were maintained in the presence of stringent 12 h light: 12 h dark cycles at 25 °C. The number of dead flies in each vial was recorded every 12 h until 100% mortality was attained. Mortality was defined as the cessation of locomotion.

Weight measurement

5- to 7-day-old adult male flies were placed in 1.5 ml microcentrifuge tubes in groups of 20. Each sample was then weighed on a Mettler AE 100 Analytical Balance.

Feeding

5- to 7-day-old adult male flies were reared on standard medium. These flies were subsequently transferred in groups of 35 to starvation vials that contained a 1% agar medium for 12 h prior to testing. A modified version of the Capillary Feeder (CAFE) assay described in Ja *et al*., (59) was used to measure ingestion of liquid food from a graduated glass microcapillary (WPI, Sarasota, FL). Briefly, flies were cold-anesthetized and transferred to empty vials with a cappilary affixed to the top as explained in Itskov and Ribiero and Masek *et al*., (47,60). Each capillary was filled with liquid food comprised of 100 mM sucrose and blue dye for visualization. The amount of food consumed every half hour was monitored by measuring the level of the meniscus of the liquid in each capillary every half hour. All recorded values were normalized to an evaporation control that contained no flies as described in Xu *et al*., (31).

Activity levels

Male flies of the appropriate genotype were collected 0–4 days post eclosion and entrained to a stringent 12 h light: 12 h dark cycle for three days at 25 °C. Flies were then placed in individual tubes containing 5% sucrose, 2% agar, and loaded into monitors (Trikinetics, DAM2 system, Waltham, MA) that were returned to a light: dark cycle at 25 °C. The activity of these flies, as indicated by beam breaks, was measured from days 2 to 6. The daily activity of each fly was averaged over the 5 days used for analysis, and the average daily activity of each genotype was determined. Flies that died at any time during the assay were excluded from analysis.

NAD^{+}/NADH quantification

The concentrations of nicotinamide nucleotides were measured using the NAD^{+}/NADH Quantification Colorimetric Kit (BioVision, Milpitas, CA) as described in Balan *et al*., (61). Briefly, adult male flies aged 5 to 7 days were collected on dry ice.

Fly heads were removed prior to homogenization and the decapitated fly bodies were pooled in groups of 10. The samples were homogenized in 400 μl of the NADH/NAD Extraction Buffer supplied in the kit and the homogenate was centrifuged at 18407 × *g* for 5 minutes at 25°C to remove debris. The cycling reaction was carried out as per the manufacturer's instructions for 2 h and the nicotinamide nucleotide concentrations were determined in duplicate. The protein concentration of each sample was measured with the Pierce® BCA Protein Assay Kit (Thermo Scientific, Rockford, IL). The concentration of nicotinamide nucleotide contained in each sample was then normalized to its respective protein content.

Mitochondrial preparation

Adult male flies aged 5 to 7 days were dissected to yield 50 thoraces per genotype. The dissected thoraces were then homogenized in a 1.5 ml micro centrifuge tube that contained 100 μl of a chilled mitochondrial isolation medium (MIM) comprised of 250 mM sucrose, 10 mM Tris-HCl pH 7.4, 0.15 mM $MgCl_2$, and a protease inhibitor cocktail (Roche, Indianapolis, IN). After careful homogenization, an additional 500 μl of MIM was added and the homogenate was centrifuged at 500 × *g* for 5 min at 4°C. The supernatant was then transferred to a fresh micro centrifuge tube and centrifuged at 5000 × *g* for 5 min at 4°C. The resultant pellet containing the crude mitochondrial fraction was washed with 500 μl MIM and resuspended in 115 μl of 1X PBS. 15 μl of this mitochondrial suspension was reserved for protein estimation using the Pierce® BCA Protein Assay Kit (Thermo Scientific, Rockford, IL). The remaining 100 μl of the mitochondrial suspension was loaded onto the Oroboros-O2k HRR chamber for further analysis.

Mitochondrial oxygen flux using high-resolution respirometry (HRR)

The mitochondrial preparations obtained from 50 fly thoraces per genotype were resuspended in MiRO5 buffer comprised of 0.5 mM EGTA, 3 mM $MgCl_2$, 60 mM K-lactobionate, 20 mM taurine, 10 mM KH_2PO_4, 20 mM Hepes, 110 mM sucrose and 1 g/L BSA essentially fatty acid free adjusted to pH 7.1 (54,62). Oxygen concentration was monitored using the OROBOROS® Oxygraph-2k (O2k, Oroboros Instruments, Innsbruck, Austria) in accordance with a previously published protocol (53). Briefly, the oxygen electrodes were calibrated as per manufacturer's instructions with an air-saturated respiration medium (MiRO5) at 25°C prior to all experiments. A substrate-uncoupler-inhibitor titration (SUIT) protocol was used to evaluate mitochondrial respiratory function. First, to each chamber Complex I substrates 5 mM pyruvate, 2 mM malate, 10 mM glutamate were added. Next, the Complex II substrate 10 mM succinate was added. To stimulate maximal oxygen flux, ADP (1–5 mM) was added after the addition of Complex I and II substrates. Next, the respiration uncoupler Carbonyl cyanide-4-(trifluoromethoxy)phenylhydrazone (CCCP) was titrated in 0.1 μM steps to obtain maximum electron transport capacity (ETC). Finally, all respiration was blocked by addition of the complex I inhibitor 0.5 μM rotenone, the complex II inhibitor 5 mM malonic acid, and the complex III inhibitor 2.5 μM antimycin A. To ensure that the mitochondrial membrane integrity was not compromised, a 10 μM cytochrome c was added in each experiment to be sure that respiration was not stimulated. The rate of oxygen consumption, termed oxygen flux, as a function of time was then normalized to the mitochondrial protein concentration of each sample. Data were analysed by DatLab software (v5.0, Oroboros Instruments, Innsbruck, Austria). All chemicals were purchased from Sigma-Aldrich, USA.

Transmission electron microscopy

Tissues for electron microscopic examination were fixed with 2.5% glutaraldehyde, 2.0% paraformaldehyde in 0.1M sodium cacodylate buffer, pH7.4, overnight at 4°C. After subsequent buffer washes, the samples were post-fixed in 2.0% osmium tetroxide for 1 h at room temperature, and then washed again in buffer followed by dH_2O. After dehydration through a graded ethanol series, the tissue was infiltrated and embedded in EMbed-812 (Electron Microscopy Sciences, Fort Washington, PA). Thin sections were stained with lead citrate and examined with a JEOL 1010 electron microscope fitted with a Hamamatsu digital camera and AMT Advantage image capture software.

Statistics

For the metabolomics data, standard statistical analyses were performed in ArrayStudio on log-transformed data. The programs R (http://cran.r-project.org/) and JMP were used for analyses that are not standard in ArrayStudio. Welch's two sample *t*-tests were used to identify biochemicals that differed significantly between genotypes. For all other experiments, the Prism software package (GraphPad Software, v7.0b) was used to generate graphs and perform statistical analyses. Unpaired *t*-tests were used to evaluate pairwise comparisons. Multiple comparisons were investigated using one-way analysis of variance (ANOVA) with post hoc Tukey tests or two-way ANOVA with a post hoc Sidak tests. The log- rank (Mantel-Cox) test was used to examine differences in starvation resistance between genotypes.

Supplementary Material

Supplementary Material is available at *HMG* online.

Acknowledgements

We thank Savapriya Ramamoorthy and the team at Metabolon, Inc for performing and analysing our metabolomics study; Raymond Meade and Biao Zuo at the Electron Microscopy Resource Laboratory at the University of Pennsylvania for assistance with our electron microscopy experiments; Larry Singh for statistical analysis, and Talya S. Kramer at the University of Pennsylvania for help with *Drosophila* husbandry.

Conflict of Interest statement. None declared.

Funding

FRAXA Research Foundation [to T.A.J]; the United States Department of Defense Autism Grant [AR1101189] to T.A.J; the National Institutes of Health [MH108592, NS021328, CA182384] to D.C.W; the United Mitochondrial Disease Foundation Research Grant [FP00020605] A.T.; the Genetics Training Grant at the University of Pennsylvania [T32GM008216], to E.D.W; and the McMorris Autism Early Intervention Initiative Fund to E.D.W. Funding to pay the Open Access publication charges for this article was provided by the FRAXA Research Foundation and Penn Orphan Disease Center.

References

1. Bhogal, B. and Jongens, T.A. (2010) Fragile X syndrome and model organisms: identifying potential routes of therapeutic intervention. *Dis. Model. Mech.*, **3**, 693–700.
2. Bardoni, B. and Mandel, J.-L. (2002) Advances in understanding of fragile X pathogenesis and FMRP function, and in identification of X linked mental retardation genes. *Curr. Opin. Genet. Dev.*, **12**, 284–293.
3. Verkerk, A.J.M.H., Pieretti, M., Sutcliffe, J.S., Fu, Y.-H., Kuhl, D.P.A., Pizzuti, A., Reiner, O., Richards, S., Victoria, M.F., Zhang, F. *et al.* (1991) Identification of a gene (FMR-1) containing a CGG repeat coincident with a breakpoint cluster region exhibiting length variation in fragile X syndrome. *Cell*, **65**, 905–914.
4. Bell, M.V., Hirst, M.C., Nakahori, Y., MacKinnon, R.N., Roche, A., Flint, T.J., Jacobs, P.A., Tommerup, N., Tranebjaerg, L., Froster-Iskenius, U. *et al.* (1991) Physical mapping across the fragile X: hypermethylation and clinical expression of the fragile X syndrome. *Cell*, **64**, 861–866.
5. Oberlé, I., Rousseau, F., Heitz, D., Kretz, C., Devys, D., Hanauer, A., Boué, J., Bertheas, M.F. and Mandel, J.L. (1991) Instability of a 550-base pair DNA segment and abnormal methylation in fragile X syndrome. *Science*, **252**, 1097–1102.
6. Sutcliffe, J.S., Nelson, D.L., Zhang, F., Pieretti, M., Caskey, C.T., Saxe, D. and Warren, S.T. (1992) DNA methylation represses FMR-1 transcription in fragile X syndrome. *Hum. Mol. Genet.*, **1**, 397–400.
7. Siomi, H., Siomi, M.C., Nussbaum, R.L. and Dreyfuss, G. (1993) The protein product of the fragile X gene, FMR1, has characteristics of an RNA-binding protein. *Cell*, **74**, 291–298.
8. Ashley, C.T., Wilkinson, K.D., Reines, D. and Warren, S.T. (1993) FMR1 protein: conserved RNP family domains and selective RNA binding. *Science*, **262**, 563–566.
9. Li, Z., Zhang, Y., Ku, L., Wilkinson, K.D., Warren, S.T. and Feng, Y. (2001) The fragile X mental retardation protein inhibits translation via interacting with mRNA. *Nucleic Acids Res.*, **29**, 2276–2283.
10. Laggerbauer, B., Ostareck, D., Keidel, E.M., Ostareck-Lederer, A. and Fischer, U. (2001) Evidence that fragile X mental retardation protein is a negative regulator of translation. *Hum. Mol. Genet.*, **10**, 329–338.
11. Darnell, J.C., Van Driesche, S.J., Zhang, C., Hung, K.Y.S., Mele, A., Fraser, C.E., Stone, E.F., Chen, C., Fak, J.J., Chi, S.W. *et al.* (2011) FMRP stalls ribosomal translocation on mRNAs linked to synaptic function and autism. *Cell*, **146**, 247–261.
12. Darnell, J.C. and Klann, E. (2013) The translation of translational control by FMRP: therapeutic targets for FXS. *Nat. Neurosci.*, **16**, 1530–1536.
13. de Vries, B.B., Halley, D.J., Oostra, B.A. and Niermeijer, M.F. (1998) The fragile X syndrome. *J. Med. Genet.*, **35**, 579–589.
14. Gould, E.L., Loesch, D.Z., Martin, M.J., Hagerman, R.J., Armstrong, S.M. and Huggins, R.M. (2000) Melatonin profiles and sleep characteristics in boys with fragile X syndrome: a preliminary study. *Am. J. Med. Genet.*, **95**, 307–315.
15. Jacquemont, S., Hagerman, R.J., Hagerman, P.J. and Leehey, M.A. (2007) Fragile-X syndrome and fragile X-associated tremor/ataxia syndrome: two faces of FMR1. *Lancet Neurol.*, **6**, 45–55.
16. Jin, P. and Warren, S.T. (2000) Understanding the molecular basis of fragile X syndrome. *Hum. Mol. Genet.*, **9**, 901–908.
17. Kidd, S. a., Lachiewicz, A., Barbouth, D., Blitz, R.K., Delahunty, C., McBrien, D., Visootsak, J. and Berry-Kravis, E. (2014) Fragile X syndrome: a review of associated medical problems. *Pediatrics*, **134**, 995–1005.
18. Bailey, D.B., Raspa, M. and Olmsted, M.G. (2010) Using a parent survey to advance knowledge about the nature and consequences of fragile X syndrome. *Am. J. Intellect. Dev. Disabil.*, **115**, 447–460.
19. de Vries, B.B., Fryns, J.P., Butler, M.G., Canziani, F., Wesby-van Swaay, E., van Hemel, J.O., Oostra, B.A., Halley, D.J. and Niermeijer, M.F. (1993) Clinical and molecular studies in fragile X patients with a Prader-Willi-like phenotype. *J. Med. Genet.*, **30**, 761–766.
20. Schrander-Stumpel, C., Gerver, W.J., Meyer, H., Engelen, J., Mulder, H. and Fryns, J.P. (1994) Prader-Willi-like phenotype in fragile X syndrome. *Clin. Genet.*, **45**, 175–180.
21. Fryns, J.P., Haspeslagh, M., Dereymaeker, A.M., Volcke, P. and Berghe, H. (2008) A peculiar subphenotype in the fra(X) syndrome: extreme obesity-short stature-stubby hands and feet-diffuse hyperpigmentation. Further evidence of disturbed hypothalamic function in the fra(X) syndrome?. *Clin. Genet.*, **32**, 388–392.
22. Hagerman, R.J., Rivera, S.M. and Hagerman, P.J. (2008) The fragile X family of disorders: a model for autism and targeted treatments. *Curr. Pediatr. Rev.*, **4**, 40–52.
23. Nowicki, S.T., Tassone, F., Ono, M.Y., Ferranti, J., Croquette, M.F., Goodlin-Jones, B. and Hagerman, R.J. (2007) The Prader-Willi phenotype of fragile X syndrome. *J. Dev. Behav. Pediatr.*, **28**, 133–138.
24. McLennan, Y., Polussa, J., Tassone, F. and Hagerman, R. (2011) Fragile x syndrome. *Curr. Genomics*, **12**, 216–224.
25. Muzar, Z., Lozano, R., Kolevzon, A. and Hagerman, R.J. (2016) The neurobiology of the Prader-Willi phenotype of fragile X syndrome. *Intractable Rare Dis. Res.*, **5**, 255–261.
26. Wan, L., Dockendorff, T.C. and Jongens, T.A. (2000) Characterization of dFMR1, a drosophila melanogaster homolog of the fragile X mental retardation protein homolog of the fragile X mental retardation protein. *Mol. Cell. Biol.*, **20**, 8536–8547.
27. Zhang, Y.Q., Bailey, a. M., Matthies, H.J., Renden, R.B., Smith, M. a., Speese, S.D., Rubin, G.M. and Broadie, K. (2001) Drosophila fragile X-related gene regulates the MAP1B homolog Futsch to control synaptic structure and function. *Cell*, **107**, 591–603.
28. Dockendorff, T.C., Su, H.S., McBride, S.M.J., Yang, Z., Choi, C.H., Siwicki, K.K., Sehgal, A. and Jongens, T.A. (2002) Drosophila lacking dfmr1 activity show defects in circadian output and fail to maintain courtship interest. *Neuron*, **34**, 973–984.
29. McBride, S.M.J., Choi, C.H., Wang, Y., Liebelt, D., Braunstein, E., Ferreiro, D., Sehgal, A., Siwicki, K.K., Dockendorff, T.C., Nguyen, H.T., McDonald, T.V. and Jongens, T.A. (2005) Pharmacological rescue of synaptic plasticity, courtship behavior, and mushroom body defects in a Drosophila model of fragile X syndrome. *Neuron*, **45**, 753–764.
30. Monyak, R.E., Emerson, D., Schoenfeld, B.P., Zheng, X., Chambers, D.B., Rosenfelt, C., Langer, S., Hinchey, P., Choi, C.H. and McDonald, T.V. (2016) Insulin signaling misregulation underlies circadian and cognitive deficits in a Drosophila fragile X model. *Mol. Psychiatry*, 10.1038/mp.2016.51.
31. Xu, K., Zheng, X. and Sehgal, A. (2008) Regulation of feeding and metabolism by neuronal and peripheral clocks in Drosophila. *Cell Metab.*, **8**, 289–300.

32. DiAngelo, J.R., Erion, R., Crocker, A. and Sehgal, A. (2011) The central clock neurons regulate lipid storage in Drosophila. *PLoS One*, **6**, e19921.
33. Davidovic, L., Navratil, V., Bonaccorso, C.M., Catania, M.V., Bardoni, B., Dumas, M. and Lyon, E.N.S. (2011) A metabolomic and systems biology perspective on the brain of the Fragile X syndrome mouse model. *Genome Res.*, **21**, 2190–2202.
34. Broughton, S.J., Piper, M.D.W., Ikeya, T., Bass, T.M., Jacobson, J., Driege, Y., Martinez, P., Hafen, E., Withers, D.J. and Leevers, S.J. (2005) Longer lifespan, altered metabolism, and stress resistance in Drosophila from ablation of cells making insulin-like ligands. *Proc. Natl. Acad. Sci. U. S. A*, **102**, 3105–3110.
35. Rulifson, E.J., Kim, S.K. and Nusse, R. (2002) Ablation of insulin-producing neurons in flies: growth and diabetic phenotypes. *Science*, **296**, 1118–1120.
36. Baker, K.D. and Thummel, C.S. (2007) Diabetic larvae and obese flies-emerging studies of metabolism in Drosophila. *Cell Metab.*, **6**, 257–266.
37. Schlegel, A. and Stainier, D.Y.R. (2007) Lessons from 'lower' organisms: what worms, flies, and zebrafish can teach us about human energy metabolism. *PLoS Genet.*, **3**, e199.
38. Arrese, E.L. and Soulages, J.L. (2010) Insect fat body: energy, metabolism, and regulation. *Annu. Rev. Entomol.*, **55**, 207–225.
39. Tabet, R., Moutin, E., Becker, J.A.J., Heintz, D., Fouillen, L., Flatter, E., Krężel, W., Alunni, V., Koebel, P., Dembélé, D. *et al.* (2016) Fragile X mental retardation protein (FMRP) controls diacylglycerol kinase activity in neurons. *Proc. Natl. Acad. Sci.*, **113**, E3619–E3628.
40. Berry-Kravis, E., Levin, R., Shah, H., Mathur, S., Darnell, J.C. and Ouyang, B. (2015) Cholesterol levels in Fragile X syndrome. *Am. J. Med. Genet. Part A*, **167**, 379–384.
41. Lisik, M.Z., Gutmajster, E., Aleksander,· and Siero, L. (2016) Low levels of HDL in fragile X syndrome patients. *Lipids*, **51**, 189–192.
42. Tabet, R., Vitale, N. and Moine, H. (2016) Fragile X syndrome: Are signaling lipids the missing culprits? *Biochimie*, **130**, 188–194.
43. McMahon, A.C. and Rosbash, M. (2016) Promiscuous or discriminating: Has the favored mRNA target of fragile X mental retardation protein been overlooked?. *Proc. Natl. Acad. Sci.USA*, **113**, 7009–7011.
44. Celestino-soper, P.B.S., Violante, S., Crawford, E.L., Luo, R., Lionel, A.C. and Delaby, E. (2010) A common X-linked inborn error of carnitine biosynthesis may be a risk factor for non-dysmorphic autism. *Proc. Natl. Acad. Sci. U. S. A*, **109**, 7974–7981.
45. Nava, C., Lamari, F., Héron, D., Mignot, C., Rastetter, a., Keren, B., Cohen, D., Faudet, a., Bouteiller, D., Gilleron, M. *et al.* (2012) Analysis of the chromosome X exome in patients with autism spectrum disorders identified novel candidate genes, including TMLHE. *Transl. Psychiatry*, **2**, e179.
46. Slocumb, M.E., Regalado, J.M., Yoshizawa, M., Neely, G.G., Masek, P., Gibbs, A.G., Keene, A.C. and Gilestro, G.F. (2015) Enhanced sleep is an evolutionarily adaptive response to starvation stress in drosophila. *PLoS One*, **10**, e0131275.
47. Masek, P., Reynolds, L. a., Bollinger, W.L., Moody, C., Mehta, A., Murakami, K., Yoshizawa, M., Gibbs, A.G. and Keene, A.C. (2014) Altered regulation of sleep and feeding contribute to starvation resistance in Drosophila. *J. Exp. Biol*, **217**, 3122–3132.
48. Bushey, D., Tononi, G. and Cirelli, C. (2009) The Drosophila fragile X mental retardation gene regulates sleep need. *J. Neurosci*, **29**, 1948–1961.
49. Tennessen, J.M., Barry, W.E., Cox, J. and Thummel, C.S. (2014) Methods for studying metabolism in Drosophila. *Methods*, **68**, 105–115.
50. Dus, M., Min, S., Keene, A.C., Lee, G.Y. and Suh, G.S.B. (2011) Taste-independent detection of the caloric content of sugar in Drosophila. *Proc. Natl. Acad. Sci. U. S. A*, **108**, 11644–11649.
51. Stein, L.R. and Imai, S.I. (2012) The dynamic regulation of NAD metabolism in mitochondria. *Trends Endocrinol. Metab.*, **23**, 420–428.
52. Yao, A., Jin, S., Li, X., Liu, Z., Ma, X., Tang, J. and Zhang, Y.Q. (2011) Drosophila FMRP regulates microtubule network formation and axonal transport of mitochondria. *Hum. Mol. Genet.*, **20**, 51–63.
53. Pesta, D. and Gnaiger, E. (2012) High-resolution respirometry: OXPHOS protocols for human cells and permeabilized fibers from small biopsies of human muscle. *Methods Mol. Biol.* 2012;**810**:25–58.
54. Votion, D.M., Gnaiger, E., Lemieux, H., Mouithys-Mickalad, A. and Serteyn, D. (2012) Physical fitness and mitochondrial respiratory capacity in horse skeletal muscle. *PLoS One*, **7**,
55. Clark, I.E., Dodson, M.W., Jiang, C., Cao, J.H., Huh, J.R., Seol, J.H., Yoo, S.J., Hay, B.A. and Guo, M. (2006) Drosophila pink1 is required for mitochondrial function and interacts genetically with parkin. **441**,
56. Lumaban, J.G. and Nelson, D.L. (2015) The Fragile X proteins Fmrp and Fxr2p cooperate to regulate glucose metabolism in mice. *Hum. Mol. Genet.*, **24**, 2175–2184.
57. Evans, A.M., DeHaven, C.D., Barrett, T., Mitchell, M. and Milgram, E. (2009) Integrated, nontargeted ultrahigh performance liquid chromatography/electrospray ionization tandem mass spectrometry platform for the identification and relative quantification of the small-molecule complement of biological systems. *Anal. Chem.*, **81**, 6656–6667.
58. DiAngelo, J.R. and Birnbaum, M.J. (2009) Regulation of fat cell mass by insulin in Drosophila melanogaster. *Mol. Cell. Biol.*, **29**, 6341–6352.
59. Ja, W.W., Carvalho, G.B., Mak, E.M., de la Rosa, N.N., Fang, A.Y., Liong, J.C., Brummel, T. and Benzer, S. (2007) Prandiology of Drosophila and the CAFE assay. *Proc. Natl. Acad. Sci. U. S. A*, **104**, 8253–8256.
60. Itskov, P.M. and Ribeiro, C. (2013) The dilemmas of the gourmet fly: the molecular and neuronal mechanisms of feeding and nutrient decision making in Drosophila. **7**, 1–13.
61. Balan, V., Miller, G.S., Kaplun, L., Balan, K., Chong, Z., Li, F., Kaplun, A., Vanberkum, M.F.A., Arking, R. and Freeman, D.C. (2008) Life Span Extension and Neuronal Cell Protection by Drosophila Nicotinamidase. *J. Biol. Chem.*, **283**, 27810–27819.
62. Gnaiger, E., Méndez, G. and Hand, S.C. (2000) High phosphorylation efficiency and depression of uncoupled respiration in mitochondria under hypoxia. TL - 97. *Proc. Natl. Acad. Sci. U. S. A*, **97**, VN-r, 11080–11085.